Ordered Nanostructures from Self-Assembly of H-Shaped Coil–Rod–Coil Molecules

Zhuoshi Wang,[1] Keli Zhong,[2] Yongri Liang,[3] Tie Chen,[1] Bingzhu Yin,[1] Myongsoo Lee,[4] Long Yi Jin[1,4]

[1]Key Laboratory for Organism Resources of the Changbai Mountain and Functional Molecules and Department of Chemistry, College of Science, Yanbian University, No. 977 Gongyuan Road, Yanji 133002, China
[2]College of Chemistry, Chemical Engineering and Food Safety, Bohai University, Jinzhou 121013, China
[3]College of Materials Science & Engineering, Beijing Institute of Petrochemical Technology, Beijing 102617, China
[4]State Key Laboratory of Supramolecular Structure and Materials, College of Chemistry, Jilin University, Changchun 130012, China
Correspondence to: L. Y. Jin (E-mail: lyjin@ybu.edu.cn) or M. Lee (E-mail: mslee@jlu.edu.cn)

ABSTRACT: A new class of π-conjugated, skewed H-shaped oligomers, consisting of biphenyl, phenylene vinylene, and phenylene ethynylene units as the rigid segment, were synthesized via Sonogashira coupling and Wittig reactions. The coil segments of these molecules were composed of poly(ethylene oxide) (PEO) or PEO with lateral methyl groups between the rod and coil segment, respectively. The experimental results revealed that the lateral methyl groups attached to the surface of the rod and coil segments dramatically influenced the self-assembling behavior of the molecules in the crystalline phase. H-shaped rod–coil molecules containing a lateral methyl group at the surface of the rod and PEO coil segments self-assemble into a two-dimensional columnar or a three-dimensional body-centered tetragonal nanostructures in the crystalline phase, whereas molecules lacking a lateral methyl group based on the PEO coil chain self-organize into lamellar or hexagonal perforated lamellar nanostructures. © 2014 Wiley Periodicals, Inc. J. Polym. Sci., Part A: Polym. Chem. **2014**, *00*, 000–000

KEYWORDS: body-centered tetragonal; coil–rod–coil; H-shaped molecule; nanostructure; SAXS; self-assembly

INTRODUCTION An important challenge in the preparation of self-assembling materials is to control the formation of supramolecular nanostructures with well-defined shapes and sizes. These advanced functional materials have remarkable potential in fields such as biochemistry, molecular electronics, biomimetic chemistry, and materials science.[1–7] Self-assembly of rod–coil block molecules in the bulk state leads to various supramolecular nanostructures, such as the one-dimensional (1D) lamellar, two-dimensional (2D) columnar, and three-dimensional (3D) bundles. These are held together by noncovalent forces, including hydrophobic and hydrophilic effects, electrostatic interactions, hydrogen bonding, and microphase segregation.[8–13] It has been reported that molecular parameters, such as the volume fraction of rod–to–coil segment, the cross-sectional area of the coil segment, or the shape of the rigid rod segment, dramatically influence the tendency of the molecules to form various nanostructures.[14–18]

Recently, ordered nanostructures in the form of T-shaped,[19–21] dumbbell,[22–26] and O-shaped[27] rod–coil molecules or copolymers have been reported by Lee and coworkers. The results imply that various supramolecular nanostructures can be constructed by controlling the molecular parameters of the different shape of rod–coil molecules.[28] One example is the filled cylindrical and hollow tubular scrolls that are formed through self-assembly of T-shaped rod–coil molecules consisting of a penta-*p*-phenylene-conjugated rod connected to a poly(propylene oxide) coil laterally attached through an imidazole linkage.[29] The authors explained that the structure of the scrolls could be controlled by adjusting the volume fraction of rod-to-coil segments of the T-shaped rod–coil molecules in the solid state. Hence, such a system has the potential for a wide range of applications in nanoscience. Although, to our knowledge, many papers reported the self-assembling behavior of the rod–coil molecular systems, there is no report concerning the synthesis

Zhuoshi Wang and Keli Zhong contributed equally to this work.

Additional Supporting Information may be found in the online version of this article.

and self-assembly of H-shaped coil–rod–coil oligomers. Therefore, the design of rod–coil molecules consisting of conjugated H-shaped rod building blocks and poly(ethylene oxide) (PEO) coil segments incorporating lateral methyl groups between the rod and coil segments is of great interest. Such molecules are able to self-assemble into various supramolecular nanostructures that can find applications in biochemistry and materials science.

With this in mind, in this work, we report the synthesis and structural analysis of H-shaped rod building block oligomers composed of biphenyl, phenylene vinylene, and phenylene ethynylene units as a rigid segment, and we investigate their self-assembling behaviors in bulk state by using differential scanning calorimetry (DSC) and small-angle X-ray scattering (SAXS).

RESULTS AND DISCUSSION

Synthesis of H-Shaped Oligomers 1 and 2

The synthetic route for H-shaped coil–rod–coil oligomers consisting of biphenyl, phenylene vinylene, and phenylene ethynylene units as a rigid segment is described in Scheme 1. Coil–rod–coil molecules **1** and **2** were successfully synthesized through the Sonogashira coupling reaction between 1,4-bis(2,5-diethynylstyryl)benzene (molecule **7**) and precursor **8**. Molecule **7** with tetraethynyl groups was prepared by the desilylation of molecules **6**. This in turn was obtained via a Sonogashira coupling reaction between 1,4-bis(5-bromo-2-iodostyryl)benzene (molecule **5**) and trimethylsilylacetylene (TMSA) with Pd/Cu as a catalyst. 1,4-Bis(5-bromo-2-iodostyryl)benzene was produced by the Wittig–Horner reaction of the phosphonate ylide **3** and 5-bromo-2-iodobenzaldehyde, using 2-aminobenzoic acid methyl ester and dimethyl terephthalate as starting materials. The reaction product containing **1** and **2** was purified using silica gel column chromatography and recycle gel permeation chromatography. The structures of molecules **1** and **2** were characterized by ^{1}H NMR and matrix-assisted laser desorption ionization time-of-flight (MALDI-TOF) mass spectroscopy (see Supporting Information) and were shown to be in full agreement with the structures presented in Scheme 1.

Structures of Bulk State

The self-assembling behavior of the H-shaped molecules **1** and **2** was investigated by means of DSC and SAXS. Figure 1 shows the DSC heating and cooling traces and the thermal transitions of the oligomers **1a** and **1b** and **2a** and **2b**. The transition temperatures determined from the DSC scans are summarized in Table 1. As shown in Table 1, the melting transition temperatures of the H-shaped molecules decrease with the increase in PEO coil length. By incorporating methyl groups into molecules **1** and **2**, the melting points of molecules **2a** and **2b** significantly decreased to values comparable with those for **1a** and **1b**. The results clearly prove that increasing the length of the flexible chain or incorporating side groups at the surface of the rod and coil leads to a reduced tendency of self-assembly of the rod segments for the construction of ordered nanostructures, subsequently

reducing the phase transition temperatures of molecules **2a** and **2b** in comparison to molecules **1a** and **1b**.

To identify the self-assembled nanostructures, SAXS experiments were performed for molecules **1** and **2**. In the crystalline phases of **1a**, the small-angle X-ray diffraction patterns show several sharp reflections, which correspond to equidistant q-spacings and, thus, index to a lamellar lattice [Fig. 2(a)]. The layer spacing at the lower temperature crystalline phase of 45.4 Å is less than the corresponding estimated stretching molecular length [61.6 Å by Corey–Pauling–Koltun (CPK) molecular model], indicative of a monolayer lamellar structure, in which the rod segments are fully interdigitated.

In contrast to **1a**, coil–rod–coil molecule **1b** based on the longer coil length displays a distinct nanostructure. The X-ray diffraction patterns of **1b** shown in Figure 2(b) can be indexed to the (100), (010), (200), and (300) planes, corresponding to a 2D oblique columnar structure with lattice constants $a = 66.4$ Å, $b = 51.4$ Å, and a characteristic angle $\gamma = 55°$. From the experimental values of the unit cell parameters (a, b, c) and the density ($\rho = 1.02$), the average number (n) of molecules per cross-sectional slice of the column is calculated to be approximately 4, according to the following equation, where M_w is the molecular weight and N_A is Avogadro's number.

$$n = (abc \times \sin\gamma) \times \rho \times N_A / M_w \qquad (1)$$

The results described above demonstrate that in the case of H-shaped rigid building blocks it is much easier to manipulate the supramolecular structure using different lengths of flexible PEO chains than in the case of the linear rod–coil molecular architecture. The tendency of a lamellar phase to transform into a 2D columnar phase is consistent with the results obtained on n-shaped rod–coil systems reported by our laboratory.[30,31] The variation in the supramolecular structure can be rationalized by considering the microphase separation between the dissimilar parts of the molecules and the space-filling requirement of the flexible PEO chains.

Molecules **2a** and **2b** were synthesized to investigate the influence of the methyl groups grafted on the surface of the rod and coil segments on the self-assembly tendency of H-shaped coil–rod–coil molecules. The SAXS patterns of molecule **2a** displayed two main peaks together with several reflections, as shown in Figure 3(a). The observed reflections can be indexed to the (101), (002), (102), (110), (112), (113), and (230) planes for 3D hexagonal symmetry (P63/mmc space group symmetry) with lattice constants $a = 62.2$ Å and $c = 81$ Å (see Table 2). An interesting point to be noted here is that the peak intensity associated with the (002) reflection appears to be the most intense, implying that the fundamental structure is lamellar. Hence, the supramolecular structure of **2a** can be characterized as a honeycomb-like crystalline layer of rod segments with in-plane hexagonal packing of coil perforations.[32] From the lattice parameters determined from the X-ray diffraction patterns and the densities of each segment, the perforation sizes are calculated to be 4.2 nm in diameter (see Supporting Information).
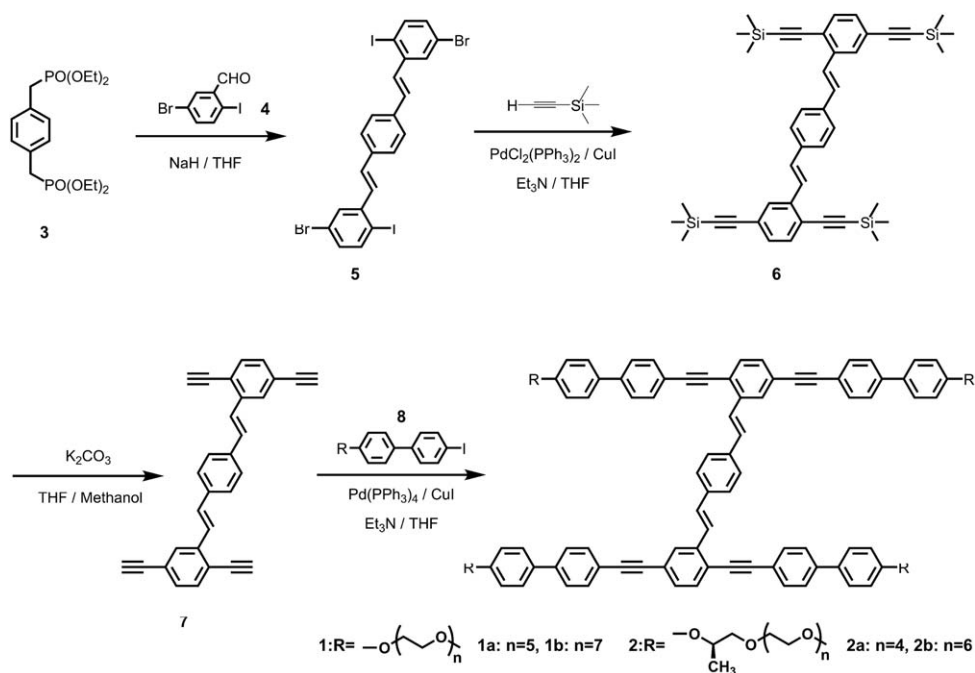
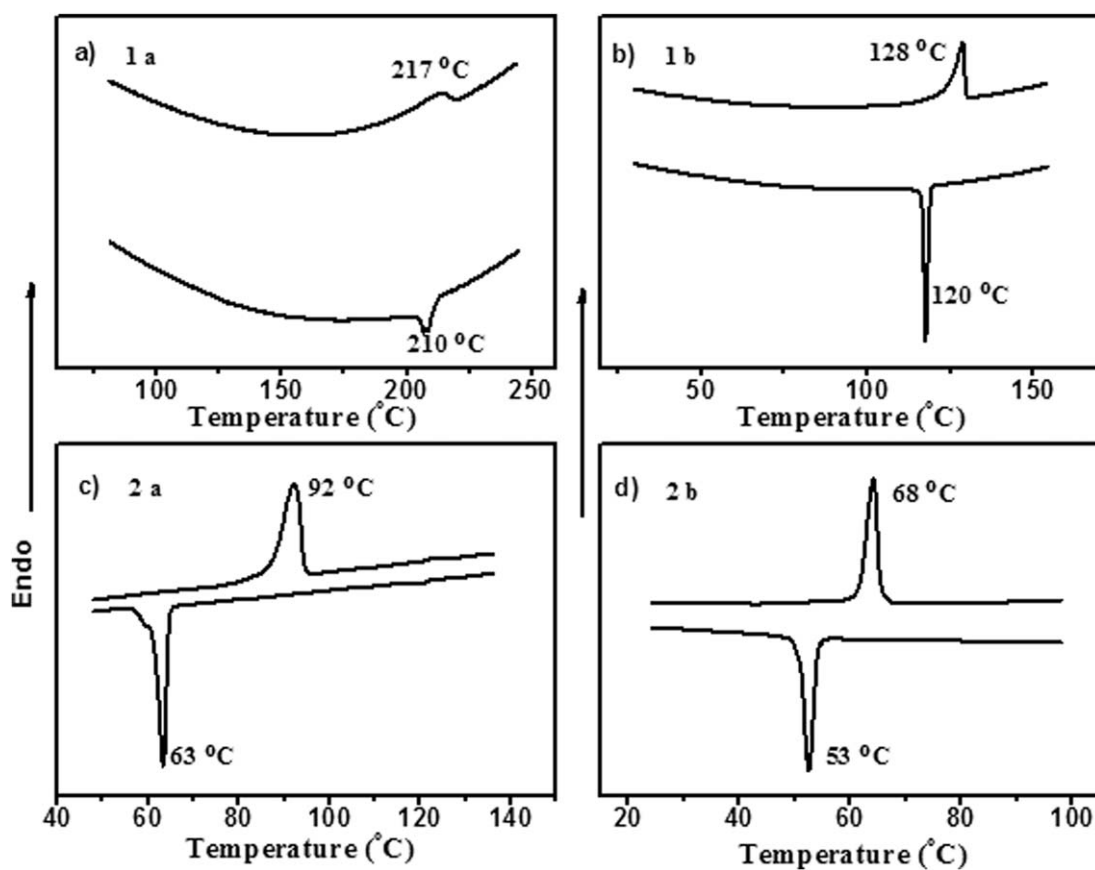**SCHEME 1** Synthetic route of H-shaped rod–coil molecules **1** and **2**.

FIGURE 1 DSC traces (10 °C/min) recorded during the second heating scan and the first cooling scan of the series of molecules **1** and **2**.

TABLE 1 Thermal Transitions and Corresponding Enthalpy Changes of Molecules **1** and **2**

Molecule	Phase Transition Temperature (°C) and Corresponding Enthalpy Changes (kJ/mol)	
	Heating	Cooling
1a	K 217 (9.3) i	i 210 (11.4) k
1b	K 128 (19.8) i	i 120 (21.3) k
2a	K 92 (20.7) i	i 63 (23.9) k
2b	K 68 (22.3) i	i 53 (24.6) k

In contrast to molecule **2a**, the SAXS patterns of molecule **2b** showed a sharp, high-intensity reflection at a low angle together with a number of sharp reflections of low intensity at higher angles [Fig. 3(b)]. These reflections can be indexed to the (110), (101), (020), (211), and (220) planes for a 3D body-centered tetragonal structure with lattice constants of $a = 69.6$ Å and $c = 64.1$ Å ($c/a = 0.92$) (see Table 3). To describe the detailed supramolecular nanostructure, it is desirable to calculate the number of molecules per micelle. From the lattice constants and the densities, the average number (n) of molecules per micelle can be calculated to be approximately 40, according to eq 2, where M_w is the molecular weight, ρ is the molecular density, and N_A is Avogadro's number.
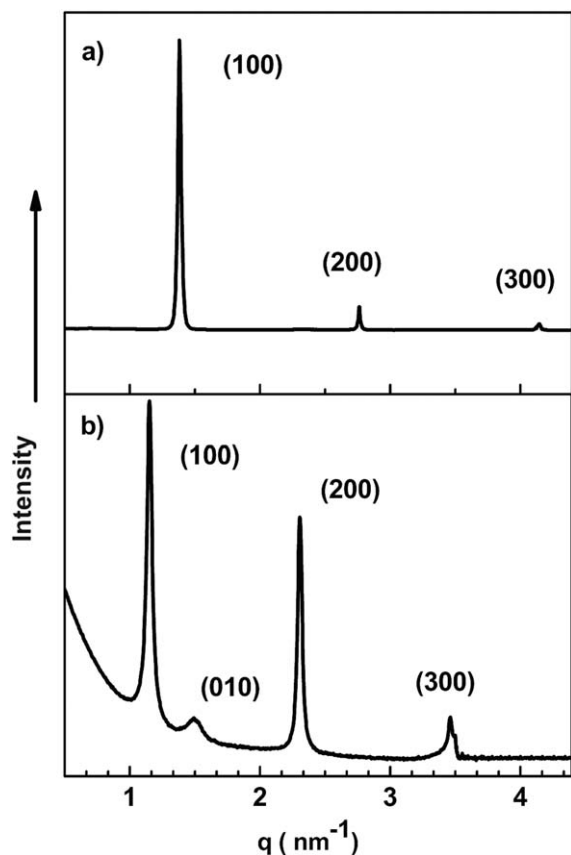
FIGURE 2 Small-angle X-ray diffraction patterns of the rod–coil oligomers **1a** and **1b** measured in their solid state.
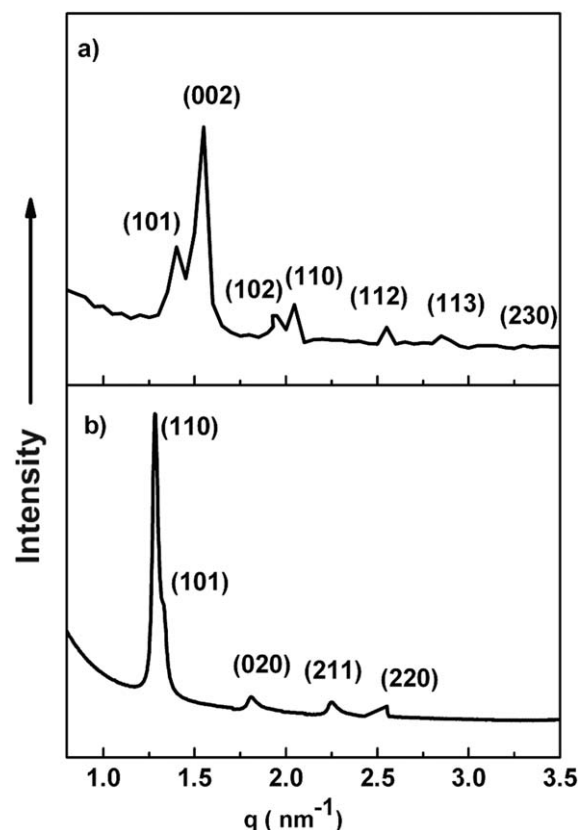
FIGURE 3 Small-angle X-ray diffraction patterns of the rod–coil oligomers **2a** and **2b** measured in their solid state.

$$n = a^2 c \frac{N_A \rho}{2 M_w} \qquad (2)$$

These results indicate that the methyl groups that are grafted on the surface of the rod and coil segments lead to the formation of various supramolecular nanostructures of the rod–coil molecular system.

On the basis of the above discussion, we reached the following conclusions. Molecules **1a** and **1b** self-assemble into a lamellar structure and an oblique columnar structure in the solid state. However, molecules **2a** and **2b**, which have lateral methyl groups at the surface of the rod and coil segments, and coil lengths identical with **1a** and **1b**, self-organize into a hexagonal perforated lamellar structure and a 3D body-centered tetragonal structure in the solid state, respectively (see Table 4). Based on the data presented so far, a schematic representation of the self-assembled structures of **1** and **2** is illustrated in Figure 4.

The structures of molecules **1a** and **2a** or **1b** and **2b**, consisting of similar rod segments and identical-length coil chains, show that the lateral methyl groups on the surface of the rod and coil segments are the main feature that influences the self-assembling behavior of coil–rod–coil molecules. The methyl groups at the surface of the rod and coil segments can lead to lower interactions of π–π stacking and, subsequently, loosen the packing of the H-shaped rod

TABLE 2 Small-Angle X-Ray Diffraction Data for Hexagonal Perforated Lamellar Structure of Molecule **2a** in the Crystalline Phase, Measured at Room Temperature

Hexagonal Perforated Lamellar Structure

h	k	l	q_{obsd} (nm^{-1})	q_{calcd} (nm^{-1})
1	0	1	1.40	1.395
0	0	2	1.55	1.552
1	1	2	2.55	2.548
1	1	3	3.05	3.051
2	0	3	5.08	5.080

q_{obsd} and q_{calcd} are the scattering vectors of the observed and calculated reflections for the hexagonal perforated lamellar structure with lattice parameters a = 6.22 nm, c = 8.1 nm (λ = 0.154 nm).

segments to produce the more stable 2D columnar or 3D bundle nanostructures (for WAXS data, see Supporting Information). Hence, the strategy of incorporating lateral methyl or short-chain alkyl groups onto the surface of rod–coil molecular systems is an effective way to construct various supramolecular nanostructures for application in nanoscience or materials science. The same is true for incorporating the lateral chain groups in the middle of the rod segment. It should be pointed out that we reported previously[16] that the lateral alkyl groups grafted on the center of the rod segment significantly to influence the self-assembling behavior of rod–coil molecules. Recently, we have constructed the hexagonal-perforate lamellar, columnar, body-centered tetragonal, and hexagonal closed-packed nanostructures with various lattice constants, by synthesizing rod–coil molecules containing lateral alkyl groups in the center of rod segments.[33,34]

CONCLUSIONS

A new class of π-conjugated, skewed H-shaped oligomers consisting of biphenyl, phenylene vinylene, and phenylene ethynylene units as a rigid segment was synthesized, via Sonogashira coupling and Wittig reactions. The coil segments of these molecules were composed of PEO or PEO with lateral

TABLE 3 Small-Angle X-Ray Diffraction Data for Body-Centered Tetragonal Structure of Molecule **2b** in the Crystalline Phase, Measured at Room Temperature

Body-Centered Tetragonal Structure

h	k	l	q_{obsd} (nm^{-1})	q_{calcd} (nm^{-1})
1	1	0	1.28	1.282
1	0	1	1.34	1.338
0	2	0	1.81	1.809
2	1	1	2.25	2.249
2	2	0	2.55	2.548

q_{obsd} and q_{calcd} are the scattering vectors of the observed and calculated reflections for the body-centered tetragonal structure with lattice parameters a = 6.96 nm, c = 6.41 nm (λ = 0.154 nm).

methyl groups between the rod and coil segment, respectively. The experimental results revealed that the lateral methyl groups grafted on the surface of the rod and coil segments dramatically influenced the self-assembling behavior in the crystalline phase. Molecule **1a**, with short coil lengths, self-assembles into a lamellar structure, while molecule **1b**, with a longer PEO coil chain, self-organizes into a 2D rectangular columnar structure. Molecules **2a** and **2b**, incorporating methyl groups between the surface of the coil and rod segments, spontaneously organize into a perforated lamellar structure and a 3D body-centered tetragonal structures, respectively. The strategy described here regarding the incorporation of methyl groups onto the surface of the rod and coil segments could induce the formation of various supramolecular nanostructures in the rod–coil molecular architecture for application in nanodevice or nanowire materials.

EXPERIMENTAL

Materials
Di(ethylene glycol) methyl ether 99%, poly(ethylene glycol)methyl ether, tetraethylene glycol 99.5%, toluene-p-sulfonyl chloride (TsCl, 98%), ($-$)-ethyl L-lactate, 3,4-dihydro-2H-pyran, 3,4-dihydro-2H-pyran (99%), p-toluenesulfonic acid monohydrate(98+%), pyridine, phosphorus tribromide, sodium hydride, tetrakis(triphenyl-phosphine)palladium (99%), copper(I) iodide (98%), triethyl phosphite, 4-hydroxy-4′-iodobiphenyl (98+%), 18-crown-6 (99%), lithium aluminum hydride (97%), methyl 2-aminobenzoate, diisobutylaluminum hydride (1 M solution in hexane), dimethyl terephthalate, pyridinium chlorochromate (98%) (all from J&K Chemical and Sigma-Aldrich), and the conventional reagents were used as received.

Techniques
^{1}H NMR spectra were recorded from CDCl$_3$ solution on a Bruker AM 300 spectrometer. Column chromatography (silica gel 100–200) was used to check the purity of the products. A Perkin Elmer Pyris Diamond differential scanning calorimeter was used to determine the thermal transitions with the maxima and minima of their endothermic or exothermic peaks, controlling the heating and cooling rates to 10 °C/min. The X-ray scattering measurements were performed in transmission mode, with synchrotron radiation at the 1W2A X-ray beam line, at the Beijing Accelerator Laboratory. The synthesized compounds powdered before preparing the XRD samples. MALDI-TOF-MS was performed on a Perceptive Biosystems Voyager-DE STR using a 2-cyano-3-(4-hydroxyphenyl) acrylic acid as matrix.

Synthesis of Precursors 3, 4, and 8
These compounds were prepared according to the procedures described elsewhere.[35,36] For detailed synthetic procedures, see Supporting Information.

Synthesis of 1,4-Bis(5-bromo-2-iodostyryl)benzene (5)
Compound **3** (0.09 g, 0.24 mmol) together with sodium hydride (0.02 mg,0.60 mmol) were put into a two-necked flask and dissolved in dry tetrahydrofuran (THF; 50 mL).

TABLE 4 Characterization of the Self-Assembling Behavior of H-Shaped Molecules **1a** and **1b** and **2a** and **2b** in the Bulk State

Molecule	f_{coil} (%)	Crystalline Phase							
		Lamellar	HPL		Oblique Columnar		Body-Centered Tetragonal	
		d (nm)	a	c	a	b	a	c
1a	50.6	4.54						
1b	58.0				6.64	5.14		
2a	51.9		6.22	8.1				
2b	60.0						6.96	6.41

f_{coil}, coil volume fraction; d, the layer spacing; HPL, hexagonal perforated layer phase; a, c, lattice constant (nm).

Upon gentle heating at 50 °C, the solution gradually turned a light yellow color. A solution of aldehyde **4** (0.11 g, 0.48 mmol) in THF (15 mL) was added dropwise over 1 h. The reaction was kept under stirring and heating for another 4 h. The small excess of sodium hydride was carefully quenched with diluted hydrochloric acid (10%, 20 mL), and the mixture was extracted several times with methylene chloride. The organic layer was dried with magnesium sulfate and concentrated under vacuum, and the crude product was purified by means of recrystallization to give the pure compound as a yellow solid (63 mg, 50%).

^{1}H NMR (300 MHz, CDCl$_3$): 7.76 (d, J = 0.9 Hz, 2H), 7.72 (d, J = 4.8 Hz, 2H), 7.58 (s, 4H), 7.26 (d, J = 9.6 Hz, 2H), 7.10 (dd, J = 5.1, 1.8 Hz, 2H), 6.98 (d, J = 9.6 Hz, 2H).

Synthesis of 1,4-Bis(2,5-bis(trimethylsilylethynyl)styryl) benzene (6)

Bis(triphenylphosphine)palladium(II) dichloride (0.53 g, 0.45 mmol) and copper iodide (0.71 g, 0.9 mmol) were added to a mixture of **5** (2.06 g, 3 mmol), trimethylsilyl acetylene (4.2 mL, 30 mmol), trimethyl amine (Et$_3$N; 5 mL), and THF (30 mL). The mixture was heated to reflux for 19 h under N$_2$
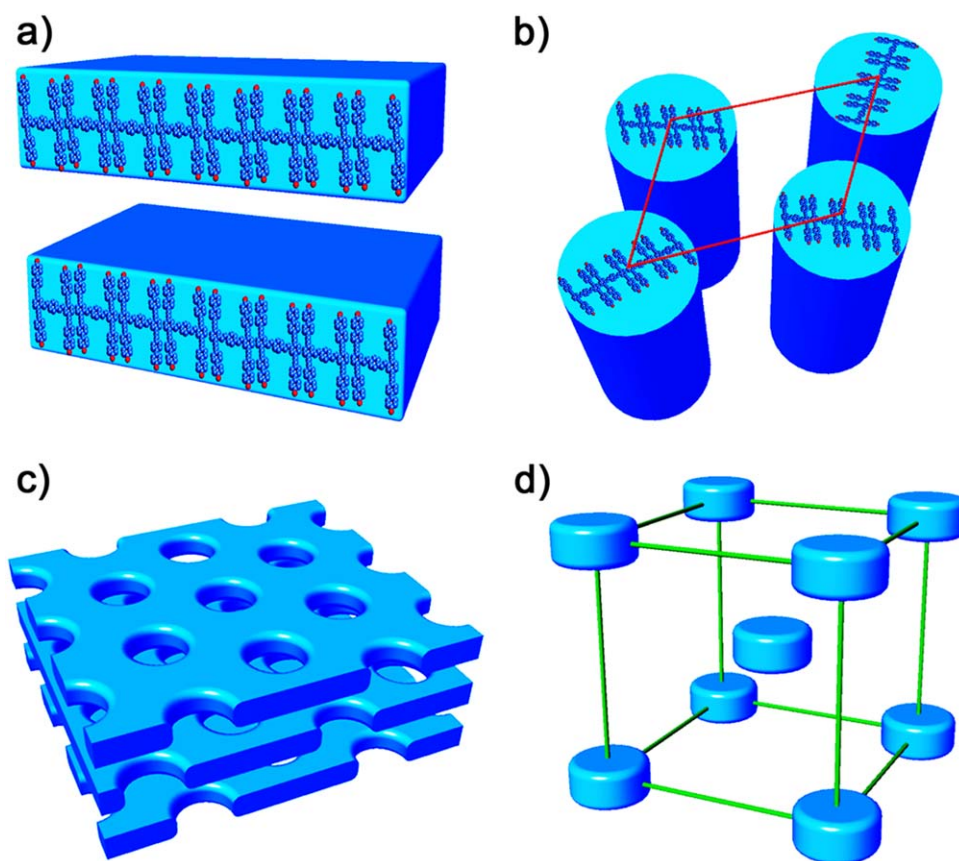

FIGURE 4 Schematic representation of self-assembly of (a) monolayer structure for **1a**, (b) oblique columnar structure for **1b**, (c) perforated lamellar structure for **2a**, and (d) body-centered tetragonal superlattice for **2b**. [Color figure can be viewed in the online issue, which is available at wileyonlinelibrary.com.]

and kept away from the light. The mixture was then diluted with methyl chloride, washed with water, and dried over $MgSO_4$. After filtration, the filtrate was concentrated to about 1.5 mL and precipitated from methanol (50 mL). The solid was collected by filtration and further purified using flash column chromatography (4:1 hexane/CH_2Cl_2) to give **6** (1.54 g, 80%) as a yellow solid.

^{1}H NMR (300 MHz, $CDCl_3$): 7.81 (s, 2H), 7.68 (d, $J = 6$ Hz, 2H), 7.57 (s, 4H), 7.44 (d, $J = 5.1$ Hz, 2H), 7.30 (dd, $J = 4.8, 0.9$ Hz, 2H), 7.22 (d, $J = 9.6$ Hz, 2H), 0.34 (s, 18H), 0.30 (s, 18H).

Synthesis of 1,4-Bis(2,5-diethynylstyryl)benzene (7)

A solution of **6** (1.54 g, 2.4 mmol) and potassium carbonate (2 g, 14.4 mmol) in THF/MeOH (30 mL/30 mL) was stirred at room temperature for 3 h. The mixture was then concentrated by evaporation and extracted with dichloromethane. The combined organic portions were dried over $MgSO_4$ and filtered. The residue was purified by flash column chromatography with 30% CH_2Cl_2 in hexanes to give product **7** (1.08 g, 91%) as a yellow solid.

^{1}H NMR (300 MHz, $CDCl_3$): 7.84 (d, $J = 0.9$ Hz, 2H), 7.62 (d, $J = 9.9$ Hz, 2H), 7.56 (s, 4H), 7.48 (d, $J = 5.1$ Hz, 2H), 7.33 (dd, $J = 4.8, 1.5$ Hz, 2H), 7.19 (d, $J = 9.9$ Hz, 2H), 3.49 (s, 2H), 3.20 (s, 2H).

Synthesis of the H-Shaped Coil–Rod–Coil Oligomers (1 and 2)

These oligomers were synthesized by the same synthetic procedures. A representative example was described for **1a**. Compound **7** (0.114 g, 0.3 mmol), compound **8** (0.954 g, 1.8 mmol), CuI (23 mg, 0.12 mmol), and Pd(PPh$_3$)$_4$ (69 mg, 0.06 mmol) were dissolved in absolute THF (30 mL) and Et$_3$N (20 mL). The mixture was refluxed for 48 h under N$_2$. Then, it was concentrated by evaporation and washed with water. The mixture was extracted with dichloroethane, dried over anhydrous magnesium sulfate, and filtered. After the solvent was removed in a rotary evaporator, the crude product was purified by silica gel chromatography (EA:CH$_3$OH, 30:1 to 10:1). The product was further purified by recycle gel permeation chromatography (JAI) to yield 0.49 g of yellow solid (25.7%).

^{1}H NMR (300 MHz, $CDCl_3$, δ, ppm): 7.84 (s, 2H), 7.72 (d, $J = 9.6$ Hz, 2H), 7.68–7.43 (m, 16 H), 7.40 (s, 4H), 7.42–7.47 (m, 12 H), 7.34 (d, $J = 9.9$ Hz, 2H), 6.67–6.70 (m, 8H), 4.20 (t, $J = 9.0$ Hz, 8H), 3.91 (t, $J = 9.0$ Hz, 8H), 3.66–3.75 (m, 64H), 3.38 (s, 12H). MALDI-TOF-MS m/z (M)$^+$ 1988, (M + Na)$^+$ 2011.

Oligomer 1b

Yield: 21.2%; ^{1}H NMR (300 MHz, $CDCl_3$, δ, ppm): 7.89 (s, 2H), 7.76 (d, $J = 9.6$ Hz, 2H), 7.72–7.68 (m, 16 H), 7.53 (s, 4H), 7.48–7.52 (m, 12 H), 7.38 (d, $J = 9.9$ Hz, 2H), 6.70–6.73 (m, 8H), 4.22 (t, $J = 9.0$ Hz, 8H), 3.93 (t, $J = 9.0$ Hz, 8H), 3.64–3.72 (m, 96H), 3.35 (s, 12H). MALDI-TOF-MS m/z (M)$^+$ 2340.

Oligomer 2a

Yield: 26.2%; ^{1}H NMR (300 MHz, $CDCl_3$, δ, ppm): 7.86 (s, 2H), 7.74 (d, $J = 9.6$ Hz, 2H), 7.68–7.72 (m, 16 H), 7.53 (s, 4H), 7.48–7.52 (m, 12 H), 7.38 (d, $J = 9.9$ Hz, 2H), 6.68–6.71 (m, 8H), 4.56–4.64 (m, 4H), 3.66–3.75 (m, 74 H), 3.37 (s, 12H), 1.35 (d, $J = 6.2$ Hz, 12H). MALDI-TOF-MS m/z (M)$^+$ 2045.

Oligomer 2b

Yield: 23.6%; ^{1}H NMR (300 MHz, $CDCl_3$, δ, ppm): 7.88 (s, 2H), 7.76 (d, $J = 9.6$ Hz, 2H), 7.70–7.74 (m, 16 H), 7.53 (s, 4H), 7.46–7.50 (m, 12 H), 7.42 (d, $J = 9.9$ Hz, 2H), 6.68–6.72 (m, 8H), 4.57–4.63 (m, 4H), 3.66–3.75 (m, 108 H), 3.34 (s, 12H), 1.35 (d, $J = 6.2$ Hz, 12H). MALDI-TOF-MS m/z (M)$^+$ 2397, (M + Na)$^+$ 2420.

REFERENCES AND NOTES

1 X. Z. Yan, T. R. Cook, J. B. Pollock, P. F. Wei, Y. Y. Zhang, Y. H. Yu, F. H. Huang, P. J. Stang, *J. Am. Chem. Soc.* **2014**, *136*, 4460-4463.

2 J. G. Hardy, *Chem. Soc. Rev.* **2013**, *42*, 7881-7899.

3 C. H. Yuan, K. Raghupathi, B. C. Popere, J. Ventura, L. Z. Dai, S. Thayumanavan, *Chem. Sci.* **2014**, *5*, 229-234.

4 S. I. Stupp, L. C. Palmer, *Chem. Mater.* **2013**, *26*, 507-518.

5 Y. Yang, Y. J. Zhang, Z. X. Wei, *Adv. Mater.* **2013**, *25*, 6039-6049.

6 X. Zhang, C. Wang, *Chem. Soc. Rev.* **2011**, *40*, 94-101.

7 T. Shimizu, M. Masuda, H. Minamikawa, *Chem. Rev.* **2005**, *105*, 1401-1444.

8 J. Heo, Y. J. Kim, M. Seo, S. Shin, S. Y. Kim, *Chem. Commun.* **2012**, *48*, 3351-3353.

9 L. Albertazzi, D. van der Zwaag, C. M. Leenders, R. Fitzner, R. W. van der Hofstad, E. Meijer, *Science* **2014**, *344*, 491-495.

10 H.-S. Sun, C.-H. Lee, C.-S. Lai, H.-L. Chen, S.-H. Tung, W.-C. Chen, *Soft Matter* **2011**, *7*, 4198.

11 Y. J. Kim, M. Seo, S. Y. Kim, *J. Polym. Sci. Part A: Polym. Chem.* **2010**, *48*, 1049-1057.

12 J. Zhang, X.-F. Chen, H.-B. Wei, X.-H. Wan, *Chem. Soc. Rev.* **2013**, *42*, 9127-9154.

13 H.-J. Kim, Y.-H. Jeong, E. Lee, M. Lee, *J. Am. Chem. Soc.* **2009**, *131*, 17371-17375.

14 J. Zhu, K. Zhong, Y. Liang, Z. Wang, T. Chen, L. Y. Jin, *Tetrahedron* **2014**, *70*, 1230-1235.

15 T. Fukino, H. Joo, Y. Hisada, M. Obana, H. Yamagishi, T. Hikima, M. Takata, N. Fujita, T. Aida, *Science* **2014**, *344*, 499-504.

16 L. Tian, K.-L. Zhong, Y. Liu, Z. Huang, L. Y. Jin, L. S. Hirst, *Soft Matter* **2010**, *6*, 5993-5998.

17 J.-H. Ryu, N.-K. Oh, W.-C. Zin, M. Lee, *J. Am. Chem. Soc.* **2004**, *126*, 3551-3558.

18 J. Ryu, B. Cho, M. Lee, *Bull. Korean Chem. Soc.* **2006**, *27*, 1270-1282.

19 J.-H. Ryu, D.-J. Hong, M. Lee, *Chem. Commun.* **2008**, 1043-1054.

20 L. Liu, K.-S. Moon, R. Gunawidjaja, E. Lee, V. V. Tsukruk, M. Lee, *Langmuir* **2008**, *24*, 3930-3936.

21 Z. Wang, J. Cui, Y. Liang, T. Chen, M. Lee, B. Yin, L. Y. Jin, *J. Polym. Sci. Part A: Polym. Chem.* **2013**, *51*, 5021-5028.

22 S. Chen, C. Ma, Z. Huang, M. Lee, *J. Phys. Chem. C* **2014**, *118*, 8181-8186.

23 J. K. Kim, E. Lee, Y. b. Lim, M. Lee, *Angew. Chem. Int. Ed.* **2008**, *47*, 4662-4666.

24 Z. Huang, J. Ryu, E. Lee, M. Lee, *Chem. Mater.* **2007**, *19*, 6569-6574.

25 E. Lee, Y. Jeong, J. Kim, M. Lee, *Macromolecules* **2007**, *40*, 8355-8360.

26 J. Ryu, H. Kim, Z. Huang, E. Lee, M. Lee, *Angew. Chem. Int. Ed.* **2006**, *45*, 5304-5307.

27 J.-H. Ryu, N.-K. Oh, M. Lee, *Chem. Commun.* **2005**, 1770.

28 K. L. Zhong, T. Chen, L. Y. Jin, *Prog. Chem.* **2012**, *24*, 1353-1358.

29 K. S. Moon, H. J. Kim, E. Lee, M. Lee, *Angew. Chem. Int. Ed.* **2007**, *46*, 6807-6810.

30 K. L. Zhong, Z. Huang, Z. Man, L. Y. Jin, B. Yin, M. Lee, *J. Polym. Sci. Part A: Polym. Chem.* **2010**, *48*, 1415-1422.

31 K. Zhong, Z. Man, Z. Huang, T. Chen, B. Yin, L. Yi Jin, *Polym. Int.* **2011**, *60*, 845-850.

32 L. Y. Jin, J. Bae, J. Ahn, M. Lee, *Chem. Commun.* **2005**, *9*, 1197-1199.

33 K.-L. Zhong, Q. Wang, T. Chen, Z. Huang, B. Yin, L. Y. Jin, *J. Appl. Polym. Sci.* **2012**, *123*, 1007-1014.

34 K.-L. Zhong, Q. Wang, T. Chen, L. Y. Jin, *Eur. Polym. J.* **2013**, *49*, 3244-3250.

35 M. Goichi, K. Segawa, S. Suzuki, S. Toyota, *Synthesis* **2005**, *2005*, 2116-2118.

36 S. Toyota, S. Suzuki, M. Goichi, *Chem.-A Eur. J.* **2006**, *12*, 2482-2487.